doi:10.1093/jmcb/mjy022
Published online May 7, 2018

Article

Lztfl1/BBS17 controls energy homeostasis by regulating the leptin signaling in the hypothalamic neurons

Qun Wei[1,2,†], Yi-Feng Gu[2,†], Qing-Jun Zhang[2], Helena Yu[2], Yan Peng[3], Kevin W. Williams[2], Ruitao Wang[4], Kajiang Yu[4], Tiemin Liu[5,*], and Zhi-Ping Liu[2,6,*]

[1] Department of Surgical Oncology and Institute of Clinical Medicine, Sir Run Run Shaw Hospital, College of Medicine, Zhejiang University, Hangzhou 310016, China
[2] Department of Internal Medicine, UT Southwestern Medical Center, Dallas, TX 75235, USA
[3] Department of Pathology, UT Southwestern Medical Center, Dallas, TX 75235, USA
[4] Department of Intensive Care Unit, The Third Affiliated Hospital, Harbin Medical University, Harbin 150081, China
[5] Sate Key Laboratory of Genetic Engineering, School of Life Sciences, Department of Endocrinology and Metabolism, Zhongshan Hospital, Collaborative Innovation Center for Genetics and Development, Fudan University, Shanghai 200438, China
[6] Department of Molecular Biology, UT Southwestern Medical Center, Dallas, TX 75235, USA
[†] These authors contributed equally to this work.
[*] Correspondence to: Tiemin Liu, E-mail: Tiemin_Liu@fudan.edu.cn; Zhi-Ping Liu, E-mail: Zhi-Ping.Liu@UTSouthwestern.edu

Edited by Feng Liu

Leptin receptor (LepRb) signaling pathway in the hypothalamus of the forebrain controls food intake and energy expenditure in response to an altered energy state. Defects in the LepRb signaling pathway can result in leptin-resistance and obesity. Leucine zipper transcription factor like 1 (Lztfl1)/BBS17 is a member of the Bardet–Biedl syndrome (BBS) gene family. Human BBS patients have a wide range of pathologies including obesity. The cellular and molecular mechanisms underlying Lztfl1-regulated obesity are unknown. Here, we generated *Lztfl1*$^{f/f}$ mouse model in which *Lztfl1* can be deleted globally and in tissue-specific manner. Global *Lztfl1* deficiency resulted in pleiotropic phenotypes including obesity. *Lztfl1*$^{-/-}$ mice are hyperphagic and showed similar energy expenditure as WT littermates. The obese phenotype of *Lztfl1*$^{-/-}$ mice is caused by the loss of *Lztfl1* in the brain but not in the adipocytes. *Lztfl1*$^{-/-}$ mice are leptin-resistant. Inactivation of *Lztfl1* abolished phosphorylation of Stat3 in the LepRb signaling pathway in the hypothalamus upon leptin stimulation. Deletion of *Lztfl1* had no effect on LepRb membrane localization. Furthermore, we observed that *Lztfl1*$^{-/-}$ mouse embryonic fibroblasts (MEFs) have significantly longer cilia than WT MEFs. We identified several proteins that potentially interact with Lztfl1. As these proteins are known to be involved in regulation of actin/cytoskeleton dynamics, we suggest that Lztfl1 may regulate leptin signaling and ciliary structure via these proteins. Our study identified Lztfl1 as a novel player in the LepRb signaling pathway in the hypothalamus that controls energy homeostasis.

Keywords: obesity, BBS, leptin-resistance, cilia, actin/cytoskeleton

Introduction

Obesity is epidemic and becoming a major public health problem worldwide. It is a major cause for the development of debilitating conditions such as type 2 diabetes, cardiovascular diseases, hypertension, and non-alcoholic steatohepatitis, all of which reduce life quality and life span. Obesity is the result of interplay among behavior, environment, and genetics. Genes related to Bardet–Biedl syndrome (BBS) are among those implicated in pathogenesis of obesity. BBS is a genetically heterogeneous autosomal recessive disorder characterized by primary features including truncal obesity, retinal degeneration, postaxial polydactyly, mental retardation, hypogenitalism and renal anomalies, and secondary features such as brachydactyl/syndactyly, reproductive and dental anomalies, and developmental delay (Sheffield, 2010; Khan et al., 2016; Suspitsin and Imyanitov, 2016). There are 20 *BBS* genes identified to date (Novas et al., 2015). Studies with mouse model of various mutant *BBS* genes revealed overlapping and unique molecular

Received November 30, 2017. Revised February 7, 2018. Accepted March 20, 2018.

and cellular mechanisms underlying the overlapping phenotypes arising from mutations in different *BBS* genes. Several *BBS* mutant mice were shown to be leptin-resistant (Rahmouni et al., 2008; Guo et al., 2016), suggesting an underlying mechanism for the obesity. However, the cellular and molecular mechanisms of the resistance remain elusive.

The BBS protein family consists of BBSome and BBSome regulators. BBSome, composed of eight BBS proteins (BBS1, 2, 4, 5, 7, 8, 9, and 18), functions as a coat complex for delivering cargo proteins to and from ciliary membrane, underlying ciliopathy phenotype of the BBS patients. Leucine zipper transcription factor like 1 (LZTFL1) was identified as BBS17 that regulates BBSome trafficking (Seo et al., 2011). *LZTFL1* mutations were found in human patients with features of BBS such as situs inversus and insertional polydactyly (Marion et al., 2012b). A strong *Lztfl1* hypomorphic mouse line was recently reported in which a gene trap cassette was introduced within the third intron (Datta et al., 2015; Jiang et al., 2016b). This mutant *Lztfl1* mouse line exhibited retinal degeneration, obesity, and ventriculomegaly, phenotypes commonly seen in other BBS mouse models. Loss of *Lztfl1* in mice was shown to result in the accumulation of non-photoreceptor outer segment (OS) proteins in the OS, suggesting dysregulation of protein trafficking being a potential mechanism for the retinal degeneration. However, the obese phenotype in Lztfl1 mutant mice was not further explored and whether Lztfl1-regulated membrane protein trafficking plays a role in obesity remains elusive. In order to identify the cellular and molecular mechanisms of Lztfl1's action, tissue-specific *Lztfl1*-deletion mouse lines are needed.

Previously, we identified a tumor suppressive function of LZTFL1 (Wei et al., 2010, 2016; Wang et al., 2014). Human *LZTFL1* gene is located at the chromosome region 3p21.3, a hotspot for tumor suppressor genes. We have shown that LZTFL1 is expressed in differentiated epithelial cells of many tissues including the stomach and lung, and downregulated in corresponding tumor tissues. Downregulation of LZTFL1 correlated with the tumor grades and metastasis, and predicted poorer survival. Re-expression of LZTFL1 in tumor cells inhibited xenograft tumor growth *in vivo* and extravasation/colonization of tumor cells to the lung (Wei et al., 2016). We found that Lztfl1 regulates not only cilia-based hedgehog signaling but also the MAPK signaling pathway. Lztfl1 is also expressed in T cells that do not have primary cilium and involved in T cell activation (Jiang et al., 2016a), suggesting that Lztfl1 may also have non-cilia-related functions. To further explore the pathophysiology of Lztfl1, we generated $Lztfl1^{f/f}$ mouse model in this study. Global *Lztfl1* deficiency resulted in obese and blind mice that were consistent with previously observed in *Lztfl1*-hypomorphic mice (Datta et al., 2015; Jiang et al., 2016b). $Lztfl1^{-/-}$ mice are hyperphagic. Furthermore, we show that the obese phenotype of $Lztfl1^{-/-}$ mice is caused by the loss of *Lztfl1* in the brain and not in the adipocytes. $Lztfl1^{-/-}$ mice are leptin-resistant. Inactivation of *Lztfl1* in the brain abolished phosphorylation of Stat3 in the LepRb signaling pathway upon leptin stimulation. Unlike *BBS2*, *BBS4*, or *BBS6* whose inactivation resulted in an altered LepR trafficking to the membrane (Seo et al., 2009), deletion of *Lztfl1* had no effect on LepRb membrane localization. Furthermore, we observed that $Lztfl1^{-/-}$ mouse embryonic fibroblasts (MEFs) have significantly longer cilia than WT MEFs. We identified several proteins that potentially interact with Lztfl1. As these proteins are known to be involved in the regulation of actin/cytoskeleton dynamics, we speculate that Lztfl1 may regulate leptin signaling and ciliary structure via these proteins.

Results

Lztfl1 mutants have pleiotropic phenotypes that are commonly seen in BBS

We used a targeting vector from knockout mouse project (KOMP) to create $Lztfl1^{1a/+}$ mice (Supplementary Figure S1A–D). Using *FLPeR*-transgenic and *CAG-cre* mice and heterozygous mating, we generated several mutant *Lztfl1* mouse lines (Figure 1A): $Lztfl1^{1a/1a}$, $Lztfl1^{1b/1b}$, $Lztfl1^{1c/1c}$($Lztfl1^{f/f}$), and $Lztfl1^{1d/1d}$($Lztfl1^{-/-}$, KO). Western blot analysis of Lztfl1 in tissues of $Lztfl1^{1a/1a}$ mice indicated that $Lztfl1^{1a/1a}$ allele is likely a null or strong hypomorph (Figure 1B). While $Lztfl1^{1c/1c}$ ($Lztfl1^{f/f}$) mice did not show any obvious phenotype and were indistinguishable from WT mice, adult mutant *Lztfl1* mice ($Lztfl1^{1a/1a}$, $Lztfl1^{1b/1b}$, *and* $Lztfl1^{-/-}$) showed similar phenotypes including retinal degeneration (Figure 1C) and obesity (Figure 1D). On examining the histology of the eyes of 3-month-old *Lztfl1* KO and WT littermates, we observed degeneration of OS of the retina and loss of photoreceptors (Figure 1C). *Lztfl1* KO mice are also born developmentally delayed even though their bodyweight catches up later on (Figure 1D). A spectrum of partial penetrate phenotypes was also observed in mutant *Lztfl1* mice, including malocclusion and vaginal atresia (Figure 1E). We also observed partial embryonic lethality for $Lztfl1^{1a/1a}$ mice as they were born significantly less-than-expected Mendelian ratio (Supplementary Figure S1E). The embryonic lethality can be traced back as early as E10.0 showing sever developmental delay (Figure 1E).

Lztfl1-null mice are obese and diabetic

We focused on the fully penetrant obese phenotype. *Lztfl1*-null mice are smaller than control littermates at birth, but catch up in bodyweight with their respective littermates around 6–8 weeks and become obese onwards (Figure 1D). However, the body length of adult Lztfl1-null mice remains significantly shorter than that of WT littermates (Figure 1D). Body fat mass composition analysis indicated that the weight gain in *Lztfl1* KO mice is due to the fat which is already significantly higher at 10 weeks compared to WT littermates when the bodyweight of both genotypes is similar (Figure 2A). Upon examining the histology of the fat tissue, we observed adipocyte hypertrophy in $Lztfl1^{-/-}$ mice (Figure 2B). Oral glucose tolerance test (OGTT) in obese 3-month-old male *Lztfl1*-null mice indicated that they have significantly elevated baseline glucose level and delayed clearance of oral glucose (Figure 2C). *Lztfl1* KO mice also have significantly decreased insulin sensitivity as indicated by insulin tolerance test (ITT) (Figure 2D). Further testing of OGTT and ITT in pre-obese 8-week-old male *Lztfl1* KO mice showed no

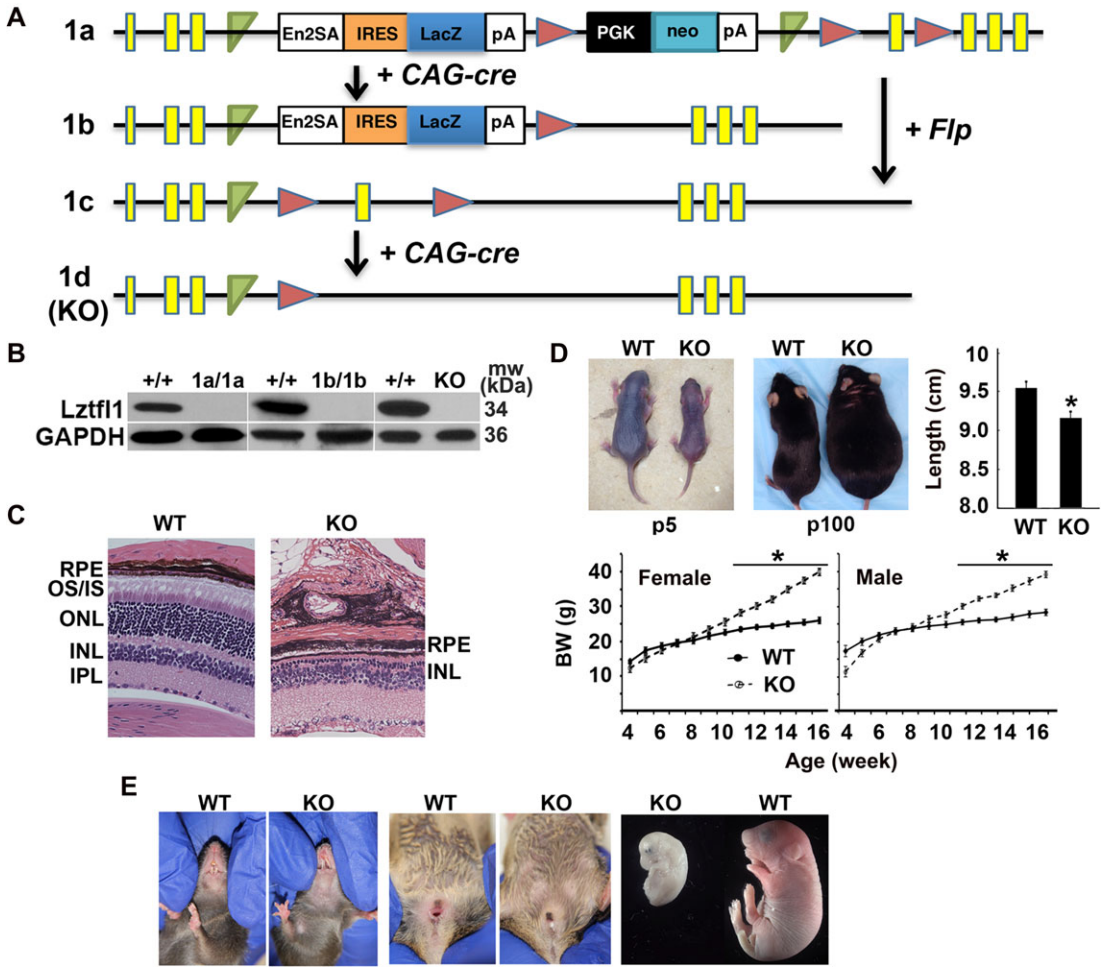

Figure 1 *Lztfl1* mutants have pleiotropic phenotypes that are commonly seen in BBS. (**A**) Schematic representation of mutant alleles of *Lztfl1*. (**B**) Western blots of brain tissue lysates showing the absence of Lztfl1 in mutant animals. (**C**) H&E staining of retina of 3-month-old WT and *Lztfl1* KO mice. (**D**) WT and *Lztfl1* KO mice at postnatal day 5 (p5) and 100 (p100). *Lztfl1* KO mice are born runt, become significantly heavier than WT littermates after postnatal week 10 (n = 10–12). At p100, *Lztfl1* KO mice also remain shorter than WT littermates. *$P < 0.05$. (**E**) Partially penetrant phenotypes of *Lztfl1* KO mice.

difference from those of WT littermates (Figure 2E and F). These results suggest that obese *Lztfl1*-null mice are diabetic and the metabolic abnormality is likely caused by obesity. Inactivation of *BBS* gene (*BBS4, BBS10, or BBS12*) *in vitro* has been shown to promote adipocyte proliferation and differentiation (Marion et al., 2012a; Aksanov et al., 2014). We tested whether Lztfl1 plays a cell autonomous role in adipocytes. We deleted *Lztfl1* in the fat tissue using *adiponectin-cre* (fKO, Supplementary Figure S2A). *Lztfl1* fKO mice were born normal that are indistinguishable with WT littermates and no adult obese phenotype was observed (Supplementary Figure S2B–D), suggesting that the obese phenotype of *Lztfl1-null* mice is due to the loss of Lztfl1 in tissue(s) other than fat.

Mice lacking Lztfl1 in the forebrain develop obesity

Since the major site of action for leptin is in the hypothalamus of the forebrain and deletion of *Lztfl1* in the fat tissue did not result in obese phenotype, we speculated that Lztfl1 may regulate the obesity via its function in the forebrain. Calcium/calmodulin-dependent protein kinase II alpha (*CamkIIα*) is expressed predominantly in the adult forebrain and male germ cells (Tsien et al., 1996; Dragatsis and Zeitlin, 2000; Choi et al., 2014). We used *CamkIIα-cre* to delete *Lztfl1* in the forebrain (camkKO) (Figure 3A). Unlike *Lztfl1* KO mice, *Lztfl1* camkKO mice were born normal without developmental delay and male mice are fertile. Like *Lztfl1* KO mice, *Lztfl1* camkKO also developed obesity at similar time point (Figure 3B). Adult *Lztfl1* camkKO mice also showed delayed clearance of oral glucose and decreased insulin sensitivity similar to that of *Lztfl1* KO mice in OGTT and ITT assays (not shown). Consistent with metabolic phenotypes, histological examination revealed that both KO and camkKO mouse livers have extensive microvesicular and macrovesicular steatosis. Both KO and camkKO mice have pancreatic hypertrophy with enlarged islets and interlobular ducts (Figure 3C). These data suggest that the obesity and related metabolic syndrome in *Lztfl1*-deficient mice are due to the function of Lztfl1 in the forebrain. Interestingly, while renal

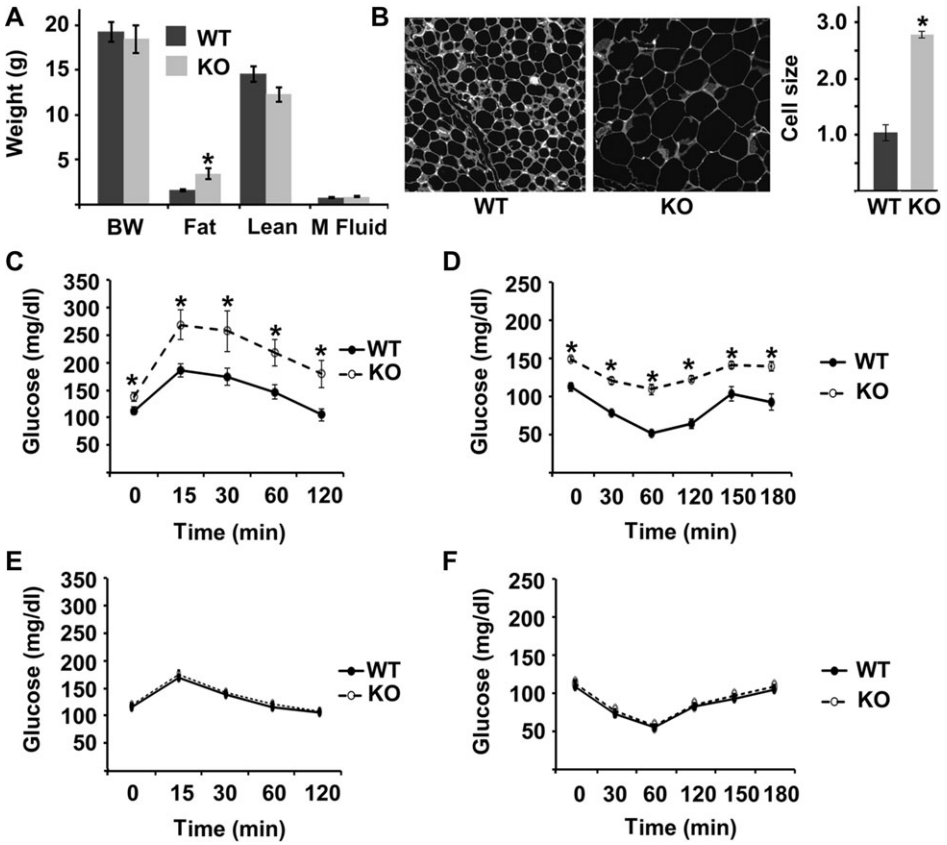

Figure 2 *Lztfl1-null* mice are obese and diabetic. (**A**) Body composition of WT and KO mice at 10 weeks of age. (**B**) Oil-red staining of WT and *Lztfl1* KO fat tissue. The size of *Lztfl1* KO adipocytes is significantly larger than that of WT ($n = 5$). *$P < 0.05$. (**C** and **D**) OGTT (**C**) and ITT (**D**) of 3-month-old male WT and *Lztfl1* KO mice ($n = 9$–12). *$P < 0.05$. (**E** and **F**) OGTT (**E**) and ITT (**F**) of 8-week-old male WT and pre-obese *Lztfl1* KO mice ($n = 8$–10). *$P < 0.05$.

abnormality is one of the primary features of BBS patients and *BBS2*$^{-/-}$ mice developed renal cysts (Nishimura et al., 2004), no gross histological abnormality was observed in *Lztfl1*$^{-/-}$ KO mice (Figure 3C).

Lztfl1-null mice are leptin-resistant and Lztfl1 is required for leptin signaling in the hypothalamus

To identify the cellular mechanism of Lztfl1-regulated obesity, we subjected *Lztfl1* KO and WT littermates to metabolic phenotyping. Inactivation of *Lztfl1* resulted in an increased food intake (Figure 4A). Yet, the energy expenditure of *Lztfl1* KO mice, as measured by heat (H) production, VO_2 and VCO_2, is similar to that of WT littermates (Figure 4B). We next tested serum leptin level in *Lztfl1*$^{-/-}$ mice at both the pre-obese and the obese stage and observed significant upregulation of leptin at both feed and fast conditions compared to WT littermates (Figure 4C), suggesting that *Lztfl1-null* mice are leptin-resistant. Because leptin regulates appetite and energy expenditure in neurons in hypothalamus, we speculated that Lztfl1 may regulate leptin signaling in the hypothalamus. We measured levels of hypothalamic orexigenic and anorexigenic neuropeptides that are involved in the regulation of energy homeostasis, no significant changes of AgRP, NPY, and POMC transcription were found between WT and *Lztfl1* KO mice, although a trend towards increased Pomc and Sosc-3 and decreased Npy was observed in *Lztfl1* KO mice (Supplementary Figure S3). Importantly, leptin-stimulated phosphorylation of Stat3 in the hypothalamus was significantly attenuated in 8-week-old pre-obese *Lztfl1* KO mice compared to WT mice (Figure 4D) upon leptin stimulation, indicating that Lztfl1 is required for leptin signaling in the hypothalamus.

Lztfl1 functions downstream of LepRb in regulation of actin/cytoskeleton dynamics

To further understand the molecular mechanism underlying Lztfl1-regulated leptin signaling, we knocked down Lztfl1 in mouse hypothalamus-derived cell line GT1-7 using Lztfl1-specific siRNAs. Consistent with the *in vivo* observation, knockdown of Lztfl1 in GT1-7 cells significantly attenuated pStat3 in response to leptin compared to control (ctl) siRNA knockdown (Figure 5A, left panel). Loss of pStat3 in GT1-7 cells with Lztfl1 knockdown in response to leptin can be rescued by ectopic overexpression of human myc-LZTFL1 (Figure 5A, lanes 7 vs. 8). The effect of Lztfl1 on pStat3 appears to be specific to lepRb/Stat3 signaling since knockdown of Lztfl1 failed to attenuate IL6 stimulated-Stat3

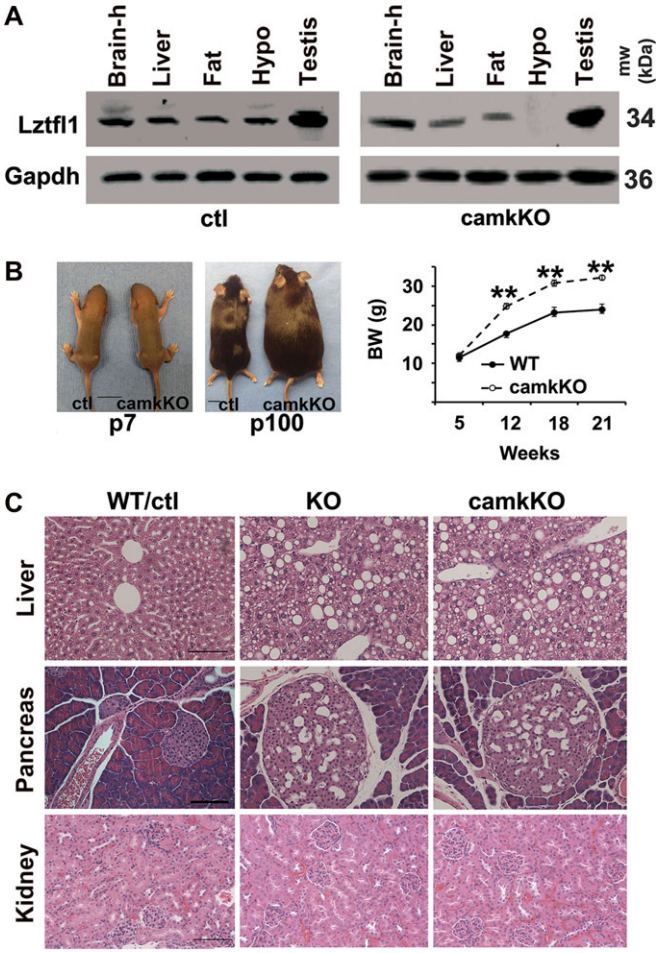

Figure 3 Deletion of *Lztfl1* in the forebrain resulted in obesity. (**A**) Western blot showing the absence of Lztfl1 in hypothalamus in *Lztfl1* camkKO mice. (**B**) *Lztfl1* camkKO and control littermate (*Lztfl1*$^{f/f}$) at postnatal day 7 (p7) and p100. *Lztfl1* camkKO mice developed obesity in adulthood. n = 10–15, $^{*}P < 0.05$. (**C**) H&E of liver, pancreas, and kidney of WT/control littermates, *Lztfl1* KO, and *Lztfl1* camkKO mice.

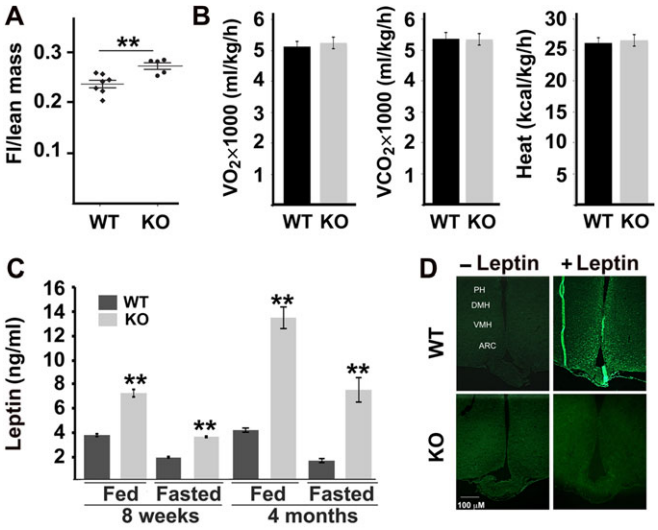

Figure 4 *Lztfl1*-null mice are hyperphagic and leptin-resistant. (**A**) Food intake of 3-month-old WT and *Lztfl1* KO male mice (n = 7–9). $^{**}P < 0.001$ by analysis of covariance. (**B**) O_2 and CO_2 consumption and heat (H) production of 3-month-old WT and *Lztfl1* KO male mice (n = 8–10). Values are normalized against lean body mass. (**C**) Serum levels of leptin in 8-week-old and 4-month-old WT and *Lztfl1* KO mice in fed and fasted states (n = 5). $^{**}P < 0.01$. (**D**) Immunofluorescence staining of pStat3 in different areas of hypothalamus of 8-week-old WT and pre-obese *Lztfl1* KO mice after vehicle PBS and leptin treatment. ARC, arcuate nucleus; VMH, ventromedial hypothalamus; DMH, dorsomedial hypothalamus; PH, posterior hypothalamic area.

phosphorylation (Figure 5A, right panel). Lztfl1 knockdown did not seem to affect leptin-stimulated ERK or CREB signaling neither (Supplementary Figure S4). We next established a stable GT1-7 cell line that expresses Flag-tagged Lztfl1 using lentiviral infection. Protein extracts from Flag-Lztfl1-expressing cells and GFP-expressing GT1-7 cells were subjected to anti-flag immunoprecipitation. The immunocomplexes were subjected to mass spectrometry to identify potential Lztfl1-interactive proteins. Approximately, 100 proteins were identified in the co-immunoprecipitates in Flag-Lztfl1-expressing GT1-7 cells but not in GFP-expressing GT1-7 cells, among them BBS1, 2, 4, 5, 7, and 9 were found as previously reported, demonstrating the validity of the experiment and specificity of the interaction (Supplementary Table S2). We also found that there is a large number of ribosomal proteins as potential Lztfl1-interactive partners. Gene ontology analysis indicated that they are involved in the biological process of co-translational protein targeting to membrane (Figure 5B), consistent with its proposed function as a coat protein for delivering cargo proteins to and from membrane (Seo et al., 2011). We tested whether *Lztfl1*-deletion may inhibit LepRb trafficking to the membrane. We biotin-labeled cell surface proteins in GT1-7^{LepRb} cells that express stably transfected myc-LepRb with Sulfo-NHS-LC-biotin using an EZ-link assay. Membrane-bound myc-LepRb in control or Lztfl1-knockdown cells in the presence or absence of leptin stimulation were isolated using avidin-beads and quantified by western blot analysis using anti-myc antibody. Knockdown of Lztfl1 did not alter the express level of overexpressed cell surface myc-lepRb significantly (Figure 5C). These results suggest that Lztfl1 may not affect LepRb upstream signaling events. That being said, it is noted that whether endogenous leptin receptor trafficking may be affected by knockdown of Lztfl1 remains to be determined since we are unable to quantify the membrane-bound endogenous LepRb due to lack of good antibodies against LepRb.

Cytoskeleton organization and actin dynamics are known to modulate Jak/Stat signaling pathways (Tamarit et al., 2013). We noticed that several actin/actin-binding proteins were among the Lztfl1-interactive partners such as Cfl2, Ktn1, kif2a, Tmp3, and Actg2. We confirmed the interaction between actin and Lztfl1 using an actin polymerization/co-sedimentation assay with purified actin and Lztfl1 (Figure 5D). These results suggest

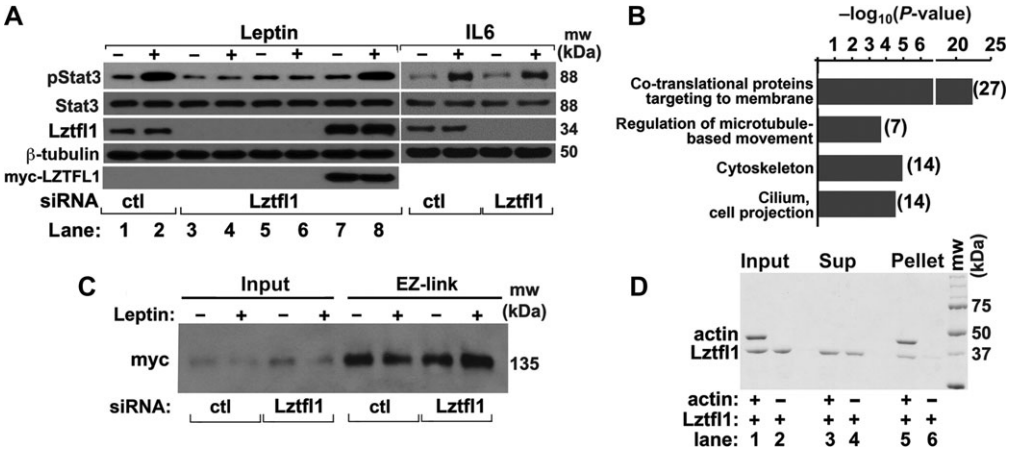

Figure 5 Lztfl1 functions downstream of the lepRb signaling pathway in the cytoskeleton compartment. (**A**) GT1-7 cells were transfected with control or Lztfl1 siRNA, stimulated with or without Leptin (100 ng/ml) (left panel) or IL6 (100 ng/ml) (right panel). In the rescue experiment, human myc-LZTFL1 was transfected along with siRNAs before Leptin stimulation. Cells were harvested 30 min later for western blot analysis with antibodies indicated. (**B**) GO analysis of proteins that interact with Lztfl1 in Flag-Lztfl1-expressing GT1-7 cells. (**C**) Western blot of membrane-bound myc-LepRb in control or Lztfl1 siRNA-transfected GT1-7$^{myc\text{-}lepRb}$ cells treated with vehicle or Leptin. (**D**) Coomassie blue staining of actin and lztfl1 from supernatant and pellet fractions in an actin co-sedimentation/polymerization assay.

that Lztfl1 may regulate downstream LepRb signaling events through actin/cytoskeleton.

Inactivation of Lztfl1 leads to defective cilia and hedgehog signaling

BBS is a model of ciliopathy (Zaghloul and Katsanis, 2009). The cilia length at the surface of hypothalamic neurons is important in the regulation of energy balance (Osorio, 2014) and appears regulated by the Leptin signaling (Han et al., 2014). To test whether Lztfl1 plays a role in cilia biogenesis, we isolated WT and *Lztfl1*$^{-/-}$ MEF cells and stained them with a cilia marker, acetyl-tubulin. *Lztfl1*$^{-/-}$ MEFs showed significantly longer cilia than WT MEFs (Figure 6A). MEF cells are known to respond to hedgehog ligand stimulation (Villavicencio et al., 2000). Upon stimulation of MEFs by the Smoothen agonist SAG, downstream effectors of the hedgehog pathway Gli1, Ptch1, and Ptch2 are upregulated. Their upregulations were significantly attenuated in *Lztfl1*$^{-/-}$ MEFs compared to that of WT (Figure 6B). Interestingly, even though the intracellular hedgehog signaling was downregulated in *Lztfl1*$^{-/-}$ MEFs, the ligand of the hedgehog pathway Shh was significantly upregulated, consistent with what we observed previously in Lztfl1-knockdown human bronchial epithelial cells (Wei et al., 2016).

Discussion

Obesity is caused by imbalance of energy metabolism. Leptin and LepRb are the major factors identified so far that control food intake and energy expenditure in response to an altered energy state. Leptin primarily acts on the arcuate nucleus neurons in the hypothalamus that suppress energy intake and stimulate energy expenditure, leading to reduction in stored body fat. Leptin-resistance in which human obese individuals are unresponsive to exogenous leptin to reduce appetite and bodyweight remains the major obstacle and challenge for leptin being used as a therapeutic agent against obesity. Leptin resistance can arise from hyperleptinemia (Knight et al., 2010), reduced leptin transport in the brain, or defects in LepRb signaling pathways in the hypothalamic neurons. Although it is possible that the leptin-resistance in *Lztfl1*-null mice may be due to the former two possibilities, our data strongly support the third one that Lztfl1 plays an essential role in the LepRb signaling pathway in the hypothalamus. (i) Deletion of *Lztfl1* leads to obese and diabetic phenotype. *Lztfl1*-null mice are hyperphagic, yet have similar energy expenditure as WT littermates despite elevated level of serum leptin, suggesting that energy imbalance may be the contributing factors to the obesity. (ii) Mechanistically, we showed that Lztfl1 is required for intracellular lepRb signaling in the hypothalamic neurons as inactivation of *Lztfl1* abolished phosphorylation of Stat3 in response to leptin specifically. (iii) Moreover, we show that specific deletion of *Lztfl1* in the hypothalamus recapitulated the obese and diabetic phenotypes seen in global *Lztfl1* knockout, indicating that Lztfl1 regulates the obesity in the hypothalamus. That being said, we noticed the caveats of using *Camkllα-cre* in our studies. Since *Camkllα-cre* are active in most neurons in the brain (hypothalamic and extra-hypothalamic structures), the role of Lztfl1 in non-hypothalamic structures cannot be ruled out. Nonetheless, the observed phenotype is consistent with hypothalamic induced obesity and metabolic syndrome.

How does Lztfl1 regulate leptin signaling? Mice lacking BBSome protein (BBS2, BBS4, or BBS6) showed similar leptin-resistance and reduced leptin-induced hypothalamic pStat3 (Seo et al., 2009). BBS1 was shown to interact with LepR and inactivation of BBS1, or BBS2, resulted in aberrant accumulation of LepR-containing vesicles in the perinuclear area, suggesting that mis-trafficking of LepR in BBSome-deficient mice may be

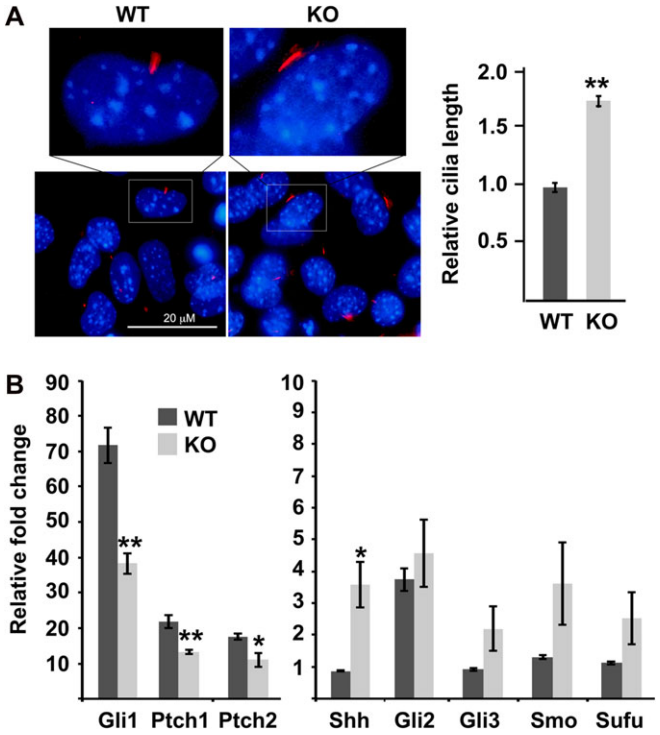

Figure 6 *Lztfl1* KO MEFs have significantly longer cilium. (**A**) MEFs from E12.5 embryos of WT and *Lztfl1* KO mice stained with acetyl-tubulin (red) and DAPI (blue) (left panel). Scale bar, 20 μm. A total of 100 individual cilia from five random chosen fields were measured using Image J and averaged. Cilia length was expressed relative to that of WT (right panel) (n = 3 independently prepped MEFs). (**B**) Confluent MEFs were serum-starved for 24 h and stimulated with (left panel) or without (right panel) SAG overnight. mRNAs of hedgehog signaling pathway components were measured by qRT-PCR and normalized against internal Gapdh and expressed as fold change relative to unstimulated cells (n = 3). *P < 0.05, **P < 0.01.

the cause of leptin-resistance (Seo et al., 2009; Guo et al., 2016). Although Lztfl1 was shown to interact with BBSome and inhibits BBsome ciliary entry (Seo et al., 2011), deletion of *Lztfl1* did not alter the expression level of membrane-bound LepR in the hypothalamic neuronal cell culture (Figure 5C), indicating that Lztfl1 may regulate leptin signaling via a novel mechanism different from that of BBSome proteins. Among the Lztfl1-interactive proteins in neuronal cells, we found that Lztfl1 interacts with actin and actin-binding proteins (Supplementary Table S2, Figure 5D). The organization of microtubules near the membrane is critical for membrane receptor signaling. Using stimulated emission depletion super-resolution optical microscopy, Tamarit et al. (2013) observed that IL-7 in CD4 T-lymphocytes induces the rapid formation of membrane microdomains, the signalosome, with dual actin-cortex organization and transient radial microtubules that bridge plasma and nuclear membrane. This microdomain regulates IL7R/JAK signaling pathway, controls Stat5 phosphorylation, transport, and translocation into the nucleus. Jiang et al. (2016a) observed that during $CD4^+$ T cell activation in contact with APC, Lztfl1 transiently redistributed to the immunological synapse, a highly organized structure of microtubules and membrane microdomains that favors directional movement of structural and signaling molecules. The immunological synapse provides equivalent primary cilia in T cells for signal molecules assemble and accumulation at the interface. Although it remains to be tested in hypothalamic neurons, we speculate that the lepRb/JAK signaling pathway may use similar signalosome to control Stat3 phosphorylation. We further speculate that Lztfl1 may interact with LepRb and couple the signalosome to the receptor since Lztfl1 knockdown attenuated the pStat3 specifically in response to Leptin but not to IL6 simulation (Figure 5A).

Our study also revealed a previously unrecognized role of Lztfl1 in cilia formation and hedgehog signaling. Global deletion of *Lztfl1* resulted in retinal degeneration and several developmental defects including embryonic lethality, malocclusion, and vaginal atresia (Figure 1E) that are commonly seen in ciliopathy. At cellular level, we observed that *Lztfl1*$^{-/-}$ MEFs have significantly longer cilium than that of WT MEFs and attenuated hedgehog signaling in response to the Smoothened agonist SAG (Figure 6). Shorter cilia were observed in *BBS4*$^{-/-}$ primary renal cells. This was attributed to elevated RhoGTPase activity that regulates the actin/cytoskeleton structure (Hernandez-Hernandez et al., 2013). The molecular mechanism by which Lztfl1 regulates the cilia length remains to be determined. Arhgef2 activates RhoGTPase by promoting the exchange of GDP for GTP. Arhgef2 was one of the proteins identified in the Lztfl1-immunopreicipitates (Supplementary Table S2). Lztfl1 may promote RhoGTPase activity via Arhgef2. *Lztfl1* deficiency may result in a decreased RhoGTPase activity, leading to lengthened cilia. Alternatively, Lztfl1 could regulate the cilia length through intraflagellar transport (IFT) system. IFT molecules are proposed to be the main regulators of ciliary growth (Keeling et al., 2016). Structural components of the cilia are delivered to the tips of the cilia and recycled to the base by the IFT system. Lztfl1 was shown to interact with IFT27. Knockdown of Lztfl1 in NIH3T3 cells caused accumulation of Smo and Patch1 in the cilia, suggesting that Lztfl1 may be required for removal of ciliary components (Eguether et al., 2014). The role of Lztfl1-regulated cilia length in obesity is a worthy subject to be further investigated in the future. Cilia on hypothalamic neurons may sense metabolic signals from the periphery to modulate ingestive behavior and energy metabolism as shortened or absence of neuronal cilia has been shown to cause obesity (Davenport et al., 2007; Han et al., 2014). We have observed longer cilia in obese *Lztfl1*-null MEFs, suggesting that maintaining proper cilia length is important for energy balance. That being said, we noted that the observed longer cilia length is in MEFs *in vitro*, whether *Lztfl1*-null mice have longer cilia in neuronal cells *in vivo* remains to be tested in the future.

While we focused on the role of Lztfl1 in the LepRb signaling pathway and associated obesity phenotype in this study, the pleiotropic phenotypes of *Lztfl1*-null mice suggest that Lztfl1 may have other roles including its tumor suppressive function and in

other signaling pathways. Indeed, some of the aged *Lztfl1*-null mice (>8 months) showed spontaneous tumors (unpublished result). It may be worthy to further investigate the significance of this observation and to test the link between diabetes and cancer risk using *Lztfl1*-null mouse model in the future.

We have identified Lztfl1 as a novel regulator of leptin signaling and obesity in hypothalamic neurons through establishing mice with *Lztfl1*-deleted globally or in forebrain tissue. Furthermore, we have identified a role of Lztfl1 in ciliary growth and hedgehog signaling. We speculate that Lztfl1 may regulate the leptin signaling and ciliary growth via its binding partners involved in actin/cytoskeleton dynamics.

Materials and methods

Generation of Lztfl1 mutants

Mouse *Lztfl1* targeting vector was from KOMP (No. CSD50165). Exon 4 of Lztfl1 in vector L3L4_pD223_DTA was flanked by two loxP sites. Linearized targeting plasmid was electroporated into JM8 ES cell line. Targeted ES cell clones were screened with Southern blot. Three positive ES cell clones were used for blastocyst injection to generate chimeric mice. High percentage chimeric mice were crossed to C57BL/6 mice to generate $Lztfl1^{1a/+}$ mice. $Lztfl1^{1a/+}$ mice were then crossed to FLPeR mice (Farley et al., 2000) to generate $Lztfl1^{f/+}$ mice. The genotype of $Lztfl1^{f/+}$ mice was detected by PCR with tail DNA. Probe sequence and PCR primers for genotyping are listed in Supplementary Table S1. *CamKII-cre* (Tsien et al., 1996; Dragatsis and Zeitlin, 2000) and *adiponectin-cre* (Eguchi et al., 2011) were used to generate conditional mice with *Lztfl1*-deleted in the brain or fat tissue, respectively. All experiments involving animals were approved by the Institutional Animal Care and Use Committee (IACUC) review boards at the UT Southwestern and performed in accordance with federal guidelines.

Body composition and metabolic studies

Conscious low-resolution nuclear magnetic resonance imaging (MRI) was used to measure body composition of mice at 10–12 weeks using EchoMRI-100™ (Echo Medical System). The activity level, food intake, volume of O_2 consumption, and volume of CO_2 production of individual mouse were measured by UT southwestern metabolic phenotyping core using CLAMS (Columbus Instruments). Heat, VO_2, and VCO_2 were calculated for dark and light cycles over a period of 7 days. Metabolic data were normalized to lean body mass (Butler and Kozak, 2010).

OGTT and ITT

For OGTT, 2- and 3-month-old male mice were fasted for 4–6 h before administration of glucose (1 g/kg bodyweight) by intragastric gavage. The blood glucose concentration was then measured at timed points using the blood collected from the tip of tail vein and an Accu-Chek glucose meter (Dacheux et al., 2015). For ITT, mice were injected with insulin (i.p. 0.5 IU/kg bodyweight, Humulin R, Eli Lilly) and blood glucose concentrations were then measured at timed points.

RNA extraction, cDNA synthesis, and qRT-PCR

Total RNA was isolated using TRIzol reagent according to the manufacturer's protocols (Life Technologies, Inc.). First-strand cDNA was made using Superscript III Reverse Transcriptase (Invitrogen). SYBR-based qRT-PCR was used to examine relative levels of selected mRNAs. All data were normalized to an internal standard (GAPDH, or Rpl19, ΔC_T method). Sequences for gene-specific primer pairs are listed in Supplementary Table S2.

Mass spectrometry analysis

GT1-7 cell lysates that stably express GFP or Lztfl1-ires-GFP were immunoprecipitated with anti-Flag antibody (M2, Sigma-Aldrich). The immunoprecipitates were washed, eluted with 100 μl 3× Flag peptide (0.2 mg/ml) (Sigma-Aldrich), and subjected for mass spectrometry.

Cell culture, MEF cells, immunoblot analysis, and EZ-link assay

GT1-7 was from ATCC. GT1-$7^{myc\text{-}LepRb}$, a stable GT1-7 cell line expressing myc-tagged leptin receptor LepRb, was a gift from Dr Liangyou Rui at University of Michigan Medical School (Su et al., 2012). GT1-7 cells that stably express Lztfl1-ires-GFP or GFP were established by infection with lentiviruses expressing Lztfl1-ires-GFP (pSin-E2F-Lztfl1-ires-GFP) and subsequent puromycin selection. GT1-7 cells were cultured in DMEM supplemented with 10% FBS. Primary MEFs were generated from embryonic day 12.5 embryos using standard protocol and cultured in Dulbecco's modified Eagle medium with 10% fetal bovine serum and penicillin/streptomycin. To activate hedgehog signaling pathway, confluent cells were treated with dimethyl sulfoxide or 100 nM SAG (Cayman Chemical) after 24 h serum starvation and incubated further for 16–20 h before harvested for western blot analysis. Antibodies were used that target pStat3 and Stat3 (#9145 and #12640, respectively, Cell Signaling Technology), Lztfl1 (Wei et al., 2010), and GAPDH (Santa Cruz). Blots were scanned, and bands were quantified using an Odyssey Licor (version 3.0) imaging system. EZ-link assays were performed on GT1-$7^{myc\text{-}lepRb}$ cells using a kit from Thermo Scientific (Thermo, #21335).

Immunofluorescence microscopy

Eight-week-old male mice were fasted for 16 h, i.p. injected with leptin (6 μg/g bodyweight) or saline, and sacrificed 30 min later. Brains were removed, dehydrated in 25% sucrose, frozen, and coronally sectioned on a microtome (30 μm). Frozen brain sections were stained with antibodies against pStat3 (#9145, Cell Signaling Technology) following the published protocol (Piper et al., 2008). For cilia staining, confluent MEF cells on coverslip were cultured in low-serum medium (0.5% FBS, 1% P/S DMEM) for 48 h. Cells were then fixed and stained with anti-acetyl-tubulin antibody (Sigma-Aldrich, T7451) following the published protocol (Dacheux et al., 2015). The length of the cilia was measured using Image J.

Statistics

All data are shown as mean ± SEM. Student's *t*-test (two-tailed) was used to compare the difference between two groups. Analysis of covariance was used for food intake and energy expenditure analysis between *Lztfl1* KO and WT littermates. $P < 0.05$ was considered statistically significant.

Supplementary material

Supplementary material is available at *Journal of Molecular Cell Biology* online.

Funding

This study was supported by the National Natural Science Foundation of China (81101581 and 81672840 to Q.W.), AHA-16GRNT3071000, NIHRO1-HL10947, and CPRIT-RP120717 to Z.-P.L.

Conflict of interest: none declared.

References

Aksanov, O., Green, P., and Birk, R.Z. (2014). BBS4 directly affects proliferation and differentiation of adipocytes. Cell. Mol. Life Sci. *71*, 3381–3392.

Butler, A.A., and Kozak, L.P. (2010). A recurring problem with the analysis of energy expenditure in genetic models expressing lean and obese phenotypes. Diabetes *59*, 323–329.

Choi, C.I., Yoon, S.P., Choi, J.M., et al. (2014). Simultaneous deletion of floxed genes mediated by CaMKIIα-Cre in the brain and in male germ cells: application to conditional and conventional disruption of Goalpha. Exp. Mol. Med. *46*, e93.

Dacheux, D., Roger, B., Bosc, C., et al. (2015). Human FAM154A (SAXO1) is a microtubule-stabilizing protein specific to cilia and related structures. J. Cell Sci. *128*, 1294–1307.

Datta, P., Allamargot, C., Hudson, J.S., et al. (2015). Accumulation of non-outer segment proteins in the outer segment underlies photoreceptor degeneration in Bardet-Biedl syndrome. Proc. Natl Acad. Sci. USA *112*, E4400–E4409.

Davenport, J.R., Watts, A.J., Roper, V.C., et al. (2007). Disruption of intraflagellar transport in adult mice leads to obesity and slow-onset cystic kidney disease. Curr. Biol. *17*, 1586–1594.

Dragatsis, I., and Zeitlin, S. (2000). CaMKIIα-Cre transgene expression and recombination patterns in the mouse brain. Genesis *26*, 133–135.

Eguchi, J., Wang, X., Yu, S., et al. (2011). Transcriptional control of adipose lipid handling by IRF4. Cell Metab. *13*, 249–259.

Eguether, T., San Agustin, J.T., Keady, B.T., et al. (2014). IFT27 links the BBSome to IFT for maintenance of the ciliary signaling compartment. Dev. Cell *31*, 279–290.

Farley, F.W., Soriano, P., Steffen, L.S., et al. (2000). Widespread recombinase expression using FLPeR (flipper) mice. Genesis *28*, 106–110.

Guo, D.F., Cui, H., Zhang, Q., et al. (2016). The BBSome controls energy homeostasis by mediating the transport of the leptin receptor to the plasma membrane. PLoS Genet. *12*, e1005890.

Han, Y.M., Kang, G.M., Byun, K., et al. (2014). Leptin-promoted cilia assembly is critical for normal energy balance. J. Clin. Invest. *124*, 2193–2197.

Hernandez-Hernandez, V., Pravincumar, P., Diaz-Font, A., et al. (2013). Bardet-Biedl syndrome proteins control the cilia length through regulation of actin polymerization. Hum. Mol. Genet. *22*, 3858–3868.

Jiang, J., Promchan, K., Jiang, H., et al. (2016b). Depletion of BBS protein LZTFL1 affects growth and causes retinal degeneration in mice. J. Genet. Genomics *43*, 381–391.

Jiang, H., Promchan, K., Lin, B.R., et al. (2016a). LZTFL1 upregulated by all-trans retinoic acid during $CD4^+$ T cell activation enhances IL-5 production. J. Immunol. *196*, 1081–1090.

Keeling, J., Tsiokas, L., and Maskey, D. (2016). Cellular mechanisms of ciliary length control. Cells *5*, pii: E6.

Khan, S.A., Muhammad, N., Khan, M.A., et al. (2016). Genetics of human Bardet-Biedl syndrome, an updates. Clin. Genet. *90*, 3–15.

Knight, Z.A., Hannan, K.S., Greenberg, M.L., et al. (2010). Hyperleptinemia is required for the development of leptin resistance. PLoS One *5*, e11376.

Marion, V., Mockel, A., De Melo, C., et al. (2012a). BBS-induced ciliary defect enhances adipogenesis, causing paradoxical higher-insulin sensitivity, glucose usage, and decreased inflammatory response. Cell Metab. *16*, 363–377.

Marion, V., Stutzmann, F., Gerard, M., et al. (2012b). Exome sequencing identifies mutations in LZTFL1, a BBSome and smoothened trafficking regulator, in a family with Bardet–Biedl syndrome with situs inversus and insertional polydactyly. J. Med. Genet. *49*, 317–321.

Nishimura, D.Y., Fath, M., Mullins, R.F., et al. (2004). Bbs2-null mice have neurosensory deficits, a defect in social dominance, and retinopathy associated with mislocalization of rhodopsin. Proc. Natl Acad. Sci. USA *101*, 16588–16593.

Novas, R., Cardenas-Rodriguez, M., Irigoin, F., et al. (2015). Bardet-Biedl syndrome: is it only cilia dysfunction? FEBS Lett. *589*, 3479–3491.

Osorio, J. (2014). Metabolism. Cilia length—role in energy balance. Nat. Rev. Endocrinol. *10*, 313.

Piper, M.L., Unger, E.K., Myers, M.G., Jr, et al. (2008). Specific physiological roles for signal transducer and activator of transcription 3 in leptin receptor-expressing neurons. Mol. Endocrinol. *22*, 751–759.

Rahmouni, K., Fath, M.A., Seo, S., et al. (2008). Leptin resistance contributes to obesity and hypertension in mouse models of Bardet-Biedl syndrome. J. Clin. Invest. *118*, 1458–1467.

Seo, S., Guo, D.F., Bugge, K., et al. (2009). Requirement of Bardet-Biedl syndrome proteins for leptin receptor signaling. Hum. Mol. Genet. *18*, 1323–1331.

Seo, S., Zhang, Q., Bugge, K., et al. (2011). A novel protein LZTFL1 regulates ciliary trafficking of the BBSome and Smoothened. PLoS Genet. *7*, e1002358.

Sheffield, V.C. (2010). The blind leading the obese: the molecular pathophysiology of a human obesity syndrome. Trans. Am. Clin. Climatol. Assoc. *121*, 172–181; discussion 181–182.

Su, H., Jiang, L., Carter-Su, C., et al. (2012). Glucose enhances leptin signaling through modulation of AMPK activity. PLoS One *7*, e31636.

Suspitsin, E.N., and Imyanitov, E.N. (2016). Bardet-Biedl syndrome. Mol. Syndromol. *7*, 62–71.

Tamarit, B., Bugault, F., Pillet, A.H., et al. (2013). Membrane microdomains and cytoskeleton organization shape and regulate the IL-7 receptor signalosome in human CD4 T-cells. J. Biol. Chem. *288*, 8691–8701.

Tsien, J.Z., Chen, D.F., Gerber, D., et al. (1996). Subregion- and cell type-restricted gene knockout in mouse brain. Cell *87*, 1317–1326.

Villavicencio, E.H., Walterhouse, D.O., and Iannaccone, P.M. (2000). The sonic hedgehog-patched-gli pathway in human development and disease. Am. J. Hum. Genet. *67*, 1047–1054.

Wang, L., Guo, J., Wang, Q., et al. (2014). LZTFL1 suppresses gastric cancer cell migration and invasion through regulating nuclear translocation of β-catenin. J. Cancer Res. Clin. Oncol. *140*, 1997–2008.

Wei, Q., Chen, Z.H., Wang, L., et al. (2016). LZTFL1 suppresses lung tumorigenesis by maintaining differentiation of lung epithelial cells. Oncogene *35*, 2655–2663.

Wei, Q., Zhou, W., Wang, W., et al. (2010). Tumor-suppressive functions of leucine zipper transcription factor-like 1. Cancer Res. *70*, 2942–2950.

Zaghloul, N.A., and Katsanis, N. (2009). Mechanistic insights into Bardet-Biedl syndrome, a model ciliopathy. J. Clin. Invest. *119*, 428–437.